Hindawi Publishing Corporation
Mathematical Problems in Engineering
Volume 2016, Article ID 5921871, 11 pages
http://dx.doi.org/10.1155/2016/5921871

Research Article

Optimal Control of Holding Motion by Nonprehensile Two-Cooperative-Arm Robot

Changan Jiang, Yuta Nakatomi, and Satoshi Ueno

Department of Mechanical Engineering, Ritsumeikan University, 1-1-1 Noji-higashi, Kusatsu, Shiga, Japan

Correspondence should be addressed to Changan Jiang; jiang@fc.ritsumei.ac.jp

Received 8 April 2016; Accepted 20 July 2016

Academic Editor: Shuhui Bi

Recently, more researchers have focused on nursing-care assistant robot and placed their hope on it to solve the shortage problem of the caregivers in hospital or nursing home. In this paper, a nonprehensile two-cooperative-arm robot is considered to realize holding motion to keep a two-rigid-link object (regarded as a care-receiver) stable on the robot arms. By applying Newton-Euler equations of motion, dynamic model of the object is obtained. In this model, for describing interaction behavior between object and robot arms in the normal direction, a viscoelastic model is employed to represent the normal forces. Considering existence of friction between object and robot arms, LuGre dynamic model is applied to describe the friction. Based on the obtained model, an optimal regulator is designed to control the holding motion of two-cooperative-arm robot. In order to verify the effectiveness of the proposed method, simulation results are shown.

1. Introduction

In recent years, with the increase of the senior citizens, the shortage problem of the caregivers appears in Japan subsequently. In order to ease caregivers' burden, many different research groups have developed some power assist devices. Among these groups, RIKEN-SRK Collaboration Center for Human-Interactive Robot Research has developed a nursing-care assistant robot named ROBEAR (see Figure 1). It was designed to lift up, hold, and transfer a person from a bed to a wheelchair or to assist a patient to stand up with its 6DOF (six degrees of freedom) arms.

Towards the more general and difficult problem of manipulating a care-receiver, this research is concerned with a simplified one: nonprehensile manipulation of a two-rigid-link object by two cooperative arms in a two-dimensional space. That is, a care-receiver is regarded as a two-rigid-link object with a passive joint. Many research works for different nonprehensile manipulation tasks can be found in the literatures [1–4]. However, these works were concerned with one-link object to be manipulated by one or two manipulators. For multilink object manipulation, [5] captured behaviors of a human and simulated for virtual human-robot interaction. To succeed in a real manipulation of a multilink object, [6] built a dynamic model for manipulating a two-rigid-link object by applying two cooperative arms and designed controllers to realize holding and lifting-up motion without considering friction. In [7], fuzzy control method was employed to compensate the effect of friction. Further, [8] proposed a control method for two cooperative arms by utilizing static friction.

Reviewing literatures related to control method for robot arms, the simplest controller is Proportional Integral Derivative (PID) feedback controller [9]. To improve the stability and tracking performance, robust control method [10–14], adaptive control method [15, 16], and sliding mode control method [17] have been applied to design appropriate controllers. In this research, considering that fast variance of movement of robot arms may lead care-receivers to feel afraid, uncomfortable, and even pained during holding and lifting-up, the designed controllers could be modified according to the care-receivers' feeling. Since optimal regulator can be modified by changing the weights which are related to state variable and control input in cost function, it could be applied to realize the holding motion of the two cooperative arms. Based on the two-rigid-link dynamic model [6, 8], [18] discussed the feasibility of guaranteeing the stability of holding motion of two-cooperative-arm robot

Figure 1: ROBEAR [21].

by using designed optimal regulator without considering friction. However, in a real-world application, the friction cannot be ignored. So, in this research, a LuGre model [19] is introduced into the dynamic model to describe friction between object and robot arms. Based on the above modified model, an approximate model around equilibrium point of the considered plant is derived. For guaranteeing the tracking performance of the system which was not considered in [18], the plant is expanded with an integrator [20] to make steady error be zero. Since the expanded plant is controllable, an optimal regulator can be designed for it according to the desired cost function. Finally, in order to verify the effectiveness of the proposed method, simulation results on holding the two-rigid-link object with two-cooperative-arm robot are shown.

The rest of this paper is organized as follows. In Section 2, problem statement is introduced. System dynamic model is presented in Section 3. In Section 4, according to the approximate model around equilibrium point, an optimal regulator is designed for holding the two-rigid-link object. Simulation results are shown in Section 5. Section 6 is conclusion of this paper.

2. Problem Statement

A schematic diagram of the system is shown in Figure 2. The object is composed of two rigid links (link 1 and link 2) which are connected by a passive joint. (x, y) is the position of the passive joint; θ_1, m_1, and I_1 and θ_2, m_2, and I_2 are the orientation angles, masses, and inertias of link 1 and link 2, respectively. The centers of mass of two links, marked as $\oplus$, are located at L_1 and L_2 from the passive joint. The object is manipulated by two arms whose positions are denoted by (x_{A1}, y_{A1}) and (x_{A2}, y_{A2}), respectively. r_1 and r_2 are the radii of two arms. l_1 and l_2 are the distances from the contact points to the passive joint. The normal forces and friction forces are acted at the contact points, which are denoted by F_{N_1}, F_{N_2} and F_{F_1}, F_{F_2}. In this paper, for holding or lifting up the object, the arms will be controlled to manipulate the object. That is, $(x_{A1}(t), y_{A1}(t))$ and $(x_{A2}(t), y_{A2}(t))$ should be controlled to guarantee that $(x(t), y(t), \theta_1(t), \theta_2(t))$ could track the desired trajectory. In order to achieve this purpose, the object dynamics model will be introduced in next section.

3. System Dynamic Model

In this section the system dynamic is considered. Employing the object dynamic model from [6, 8, 18], the dynamics of the object can be described by applying Newton-Euler equations of motion as

$$M(q)\ddot{q} + C(q,\dot{q})\dot{q} + G(q) = B_1 F_N + B_2 F_F = \tau, \quad (1)$$

where $s_i = \sin\theta_i$, $c_i = \cos\theta_i$, $q := (x, y, \theta_1, \theta_2)^T$, $F_N = (F_{N_1}, F_{N_2})^T$, $F_F = (F_{F_1}, F_{F_2})^T$,

$$\begin{aligned}
M(q) &= \begin{bmatrix} m_1+m_2 & 0 & -m_1L_1s_1 & -m_2L_2s_2 \\ 0 & m_1+m_2 & m_1L_1c_1 & m_2L_2c_2 \\ -m_1L_1s_1 & m_1L_1c_1 & I_1+m_1L_1^2 & 0 \\ -m_2L_2s_2 & m_2L_2c_2 & 0 & I_2+m_2L_2^2 \end{bmatrix}, \\
C(q,\dot{q}) &= \begin{bmatrix} 0 & 0 & -m_1L_1\dot{\theta}_1c_1 & -m_2L_2\dot{\theta}_2c_2 \\ 0 & 0 & -m_1L_1\dot{\theta}_1s_1 & -m_2L_2\dot{\theta}_2s_2 \\ 0 & 0 & 0 & 0 \\ 0 & 0 & 0 & 0 \end{bmatrix}, \\
G(q) &= \begin{bmatrix} 0 \\ (m_1+m_2)g \\ m_1gL_1c_1 \\ m_2gL_2c_2 \end{bmatrix}, \\
B_1 &= \begin{bmatrix} s_1 & -s_2 \\ -c_1 & c_2 \\ -l_1 & 0 \\ 0 & l_2 \end{bmatrix}, \\
B_2 &= \begin{bmatrix} -c_1 & c_2 \\ -s_1 & s_2 \\ 0 & 0 \\ 0 & 0 \end{bmatrix},
\end{aligned} \quad (2)$$

and g is the gravitational acceleration.

In [6], a viscoelastic model was employed to describe interaction behavior between links and arms in the normal direction (see Figure 3). In this research, the same viscoelastic model in (3) is applied to the normal forces F_{N_i}.

$$F_{N_i} = \begin{cases} k_i\delta_i + d_i\dot{\delta}_i & \text{for } \delta_i \geq 0 \\ 0 & \text{for } \delta_i < 0, \end{cases} \quad (3)$$

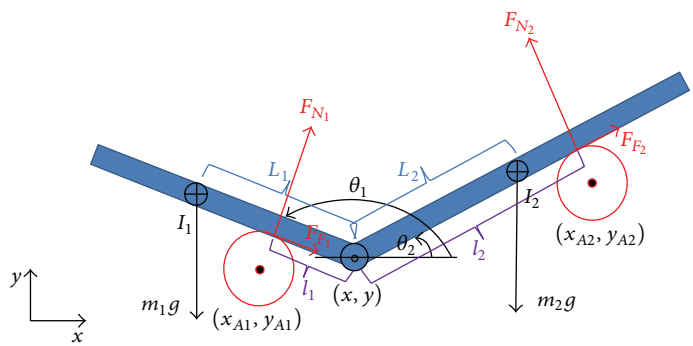

Figure 2: Schematic diagram of the system.

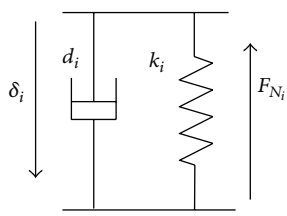

Figure 3: Viscoelastic model.

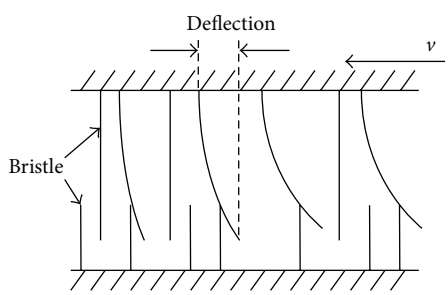

Figure 4: Sketch of LuGre model.

where k_i and d_i are spring constants and viscosity coefficient, respectively. δ_i are deformation in the normal direction at contact points. According to the geometrical relationship between links and arms, l_i and δ_i can be described as follows:

$$\begin{bmatrix} \delta_1 \\ l_1 \\ \delta_2 \\ l_2 \end{bmatrix} = -\begin{bmatrix} s_1 & -c_1 & 0 & 0 \\ c_1 & s_1 & 0 & 0 \\ 0 & 0 & s_2 & -c_2 \\ 0 & 0 & -c_2 & -s_2 \end{bmatrix} \begin{bmatrix} x - x_{A1} \\ y - y_{A1} \\ x_{A2} - x \\ y_{A2} - y \end{bmatrix} + \begin{bmatrix} r_1 \\ 0 \\ r_2 \\ 0 \end{bmatrix}. \quad (4)$$

In order to describe the friction forces between links and arms, LuGre model [19] which is based on the average deflection of the bristles between two surfaces is employed in this research. The sketch of LuGre model is shown in Figure 4 and the friction forces are defined as

$$F_{F_i} = \sigma_{0i} z_i + \sigma_{1i} \dot{z}_i - \sigma_{2i} v_i \operatorname{sgn}(v_i), \quad (5)$$

where σ_{0i}, σ_{1i}, and σ_{2i} are stiffness, damping, and viscous friction coefficients, respectively. z_i are average deflection of the bristles and represented as

$$\dot{z}_i = -v_i - \frac{|v_i|}{f(v_i)} z_i, \quad (6)$$

$$\sigma_{0i} f(v_i) = \left(\mu_{Ci} + (\mu_{Si} - \mu_{Ci}) e^{-|v_i/v_{\mathrm{st}i}|^{1/2}}\right) F_{N_i}, \quad (7)$$

where μ_{Ci} and μ_{Si} are coefficients of Coulomb friction and static friction, respectively. $v_{\mathrm{st}i}$ are the Stribeck velocities. v_i are relative velocities in the tangent direction between links and arms and represented as

$$\begin{aligned} v_1 &= -(\dot{x} - \dot{x}_{A1}) \cos\theta_1 - (\dot{y} - \dot{y}_{A1}) \sin\theta_1, \\ v_2 &= (\dot{x} - \dot{x}_{A2}) \cos\theta_2 + (\dot{y} - \dot{y}_{A2}) \sin\theta_2. \end{aligned} \quad (8)$$

4. Optimal Regulator Design

In the above section, the dynamic model of the considered system was introduced. According to the obtained nonlinear model, for specified F_{N_i} and F_{F_i}, if there exists q which can satisfy (1) when $\ddot{q} = \dot{q} = 0$, we call the state q an equilibrium point of the system. Before designing optimal regulator, a linear approximation to the obtained nonlinear model around an equilibrium point will be firstly found.

We assume that friction forces $F_{F_i} = 0$ and positions of arms as (x_{Ai0}, y_{Ai0}) when the system is at the equilibrium point $q = q_0 = (x_0, y_0, \theta_{10}, \theta_{20})^T$, $\Delta q = (\Delta x, \Delta y, \Delta\theta_1, \Delta\theta_2)^T$ is minor change from the equilibrium point, and

$$\begin{aligned} \sin\Delta\theta_i &= \Delta\theta_i, \\ \cos\Delta\theta_i &= 1, \\ \sin(\theta_{i0} + \Delta\theta_i) &= \sin\theta_{i0} + \cos\theta_{i0} \cdot \Delta\theta_i, \\ \cos(\theta_{i0} + \Delta\theta_i) &= \cos\theta_{i0} - \sin\theta_{i0} \cdot \Delta\theta_i. \end{aligned} \quad (9)$$

Then, substitute $q = q_0 + \Delta q$ into (1);

$$\tau_0 + \Delta\tau = M(q_0 + \Delta q)\,\Delta\ddot{q} + C\left(q_0 + \Delta q, \Delta\dot{q}\right)\Delta\dot{q} + G(q_0 + \Delta q) \tag{10}$$

is obtained, where $M(q_0 + \Delta q) = M(q_0) + \Delta M$, $G(q_0 + \Delta q) = G(q_0) + \Delta G$, and

$$\Delta M = \begin{bmatrix} 0 & 0 & -m_1L_1c_{10}\Delta\theta_1 & -m_2L_2c_{20}\Delta\theta_2 \\ 0 & 0 & -m_1L_1s_{10}\Delta\theta_1 & -m_2L_2s_{20}\Delta\theta_2 \\ -m_1L_1c_{10}\Delta\theta_1 & -m_1L_1s_{10}\Delta\theta_1 & 0 & 0 \\ -m_2L_2c_{20}\Delta\theta_2 & -m_2L_2s_{20}\Delta\theta_2 & 0 & 0 \end{bmatrix},$$

$$C\left(q_0 + \Delta q, \Delta\dot{q}\right) = \begin{bmatrix} 0 & 0 & -m_1L_1\Delta\dot{\theta}_1\left(c_{10} - s_{10}\Delta\theta_1\right) & -m_2L_2\Delta\dot{\theta}_2\left(c_{20} - s_{20}\Delta\theta_2\right) \\ 0 & 0 & -m_1L_1\Delta\dot{\theta}_1\left(s_{10} + c_{10}\Delta\theta_1\right) & -m_2L_2\Delta\dot{\theta}_2\left(s_{20} + c_{20}\Delta\theta_2\right) \\ 0 & 0 & 0 & 0 \\ 0 & 0 & 0 & 0 \end{bmatrix}, \tag{11}$$

$$\Delta G = \begin{bmatrix} 0 \\ 0 \\ -m_1gL_1s_{10}\Delta\theta_1 \\ -m_2gL_2s_{20}\Delta\theta_2 \end{bmatrix}.$$

Let $\Delta \cdot \Delta = 0$, $\Delta \cdot \dot{\Delta} = 0$, $\Delta \cdot \ddot{\Delta} = 0$, and then (10) becomes

$$M(q_0)\,\Delta\ddot{q} + G(q_0) + \Delta G = \tau_0 + \Delta\tau. \tag{12}$$

Since $G(q_0) = \tau_0$ when the system is stationary at equilibrium point, (12) can be simplified as

$$M(q_0)\,\Delta\ddot{q} + \Delta G = \Delta\tau. \tag{13}$$

According to (1), we can get

$$\Delta\tau = \begin{bmatrix} c_{10}\Delta\theta_1 & -c_{20}\Delta\theta_2 & 0 & 0 \\ s_{10}\Delta\theta_1 & -s_{20}\Delta\theta_2 & 0 & 0 \\ 0 & 0 & 0 & 0 \\ 0 & 0 & 0 & 0 \end{bmatrix}\begin{bmatrix} F_{N_1} \\ F_{N_2} \\ F_{N_1}l_1 \\ F_{N_2}l_2 \end{bmatrix} + \begin{bmatrix} -s_{10}\Delta\theta_1 & -s_{20}\Delta\theta_2 \\ -c_{10}\Delta\theta_1 & c_{20}\Delta\theta_2 \\ 0 & 0 \\ 0 & 0 \end{bmatrix}\begin{bmatrix} F_{F_1} \\ F_{F_2} \end{bmatrix} + \begin{bmatrix} s_{10} & -s_{20} & 0 & 0 \\ -c_{10} & c_{20} & 0 & 0 \\ 0 & 0 & -1 & 0 \\ 0 & 0 & 0 & 1 \end{bmatrix}\begin{bmatrix} \Delta F_{N_1} \\ \Delta F_{N_2} \\ \Delta\left\{F_{N_1}l_1\right\} \\ \Delta\left\{F_{N_2}l_2\right\} \end{bmatrix} + \begin{bmatrix} -c_{10} & c_{20} \\ -s_{10} & s_{20} \\ 0 & 0 \\ 0 & 0 \end{bmatrix}\begin{bmatrix} \Delta F_{F_1} \\ \Delta F_{F_2} \end{bmatrix}. \tag{14}$$

In this research, we assume that $d_i\dot{\delta}_i \approx 0$, so we get

$$\begin{bmatrix} \Delta F_{N_1} \\ \Delta F_{N_2} \\ \Delta\left\{F_{N_1}l_1\right\} \\ \Delta\left\{F_{N_2}l_2\right\} \end{bmatrix} = \begin{bmatrix} k_1 & 0 & 0 & 0 \\ 0 & 0 & k_2 & 0 \\ k_1l_1 & k_1\delta_1 & 0 & 0 \\ 0 & 0 & k_2l_2 & k_2\delta_2 \end{bmatrix}\begin{bmatrix} \Delta\delta_1 \\ \Delta l_1 \\ \Delta\delta_2 \\ \Delta l_2 \end{bmatrix}. \tag{15}$$

From (4),

$$\begin{bmatrix} \Delta\delta_1 \\ \Delta l_1 \\ \Delta\delta_2 \\ \Delta l_2 \end{bmatrix} = -\begin{bmatrix} -s_{10} & c_{10} & 0 & 0 \\ -c_{10} & -s_{10} & 0 & 0 \\ 0 & 0 & s_{20} & -c_{20} \\ 0 & 0 & -c_{20} & -s_{20} \end{bmatrix} \begin{bmatrix} \Delta x_{A1} \\ \Delta y_{A1} \\ \Delta x_{A2} \\ \Delta y_{A2} \end{bmatrix}$$
$$- \begin{bmatrix} s_{10} & -c_{10} & (x_0 - x_{A10}) c_{10} + (y_0 - y_{A10}) s_{10} & 0 \\ c_{10} & s_{10} & -(x_0 - x_{A10}) s_{10} + (y_0 - y_{A10}) c_{10} & 0 \\ -s_{20} & c_{20} & 0 & (x_{A20} - x_0) c_{20} + (y_{A20} - y_0) s_{20} \\ c_{20} & s_{20} & 0 & (x_{A20} - x_0) s_{20} - (y_{A10} - y_0) c_{20} \end{bmatrix} \begin{bmatrix} \Delta x \\ \Delta y \\ \Delta\theta_1 \\ \Delta\theta_2 \end{bmatrix} \tag{16}$$

can be obtained. Linearize (6) around $z_i = 0$ and $v_i = 0$; we can get $\dot{z}_i = -v_i$ and

$$\begin{bmatrix} \Delta F_{F_1} \\ \Delta F_{F_2} \end{bmatrix} = \begin{bmatrix} \sigma_{01} c_{10} & \sigma_{01} s_{10} & a & 0 \\ -\sigma_{02} c_{20} & -\sigma_{02} s_{20} & 0 & b \end{bmatrix} \begin{bmatrix} \Delta x \\ \Delta y \\ \Delta\theta_1 \\ \Delta\theta_2 \end{bmatrix}$$
$$+ \begin{bmatrix} \alpha c_{10} & \alpha s_{10} & 0 & 0 \\ -\beta c_{2_0} & -\beta s_{20} & 0 & 0 \end{bmatrix} \begin{bmatrix} \Delta\dot{x} \\ \Delta\dot{y} \\ \Delta\dot{\theta}_1 \\ \Delta\dot{\theta}_2 \end{bmatrix}, \tag{17}$$

where a, b, α, and β are shown as follows:

$$a = \begin{cases} -\sigma_{01}(x_0 - x_{A10}) s_{10} - (\sigma_{11} + \sigma_{21})(\dot{x} - \dot{x}_{A1}) s_{10} + \sigma_{01}(y_0 - y_{A10}) c_{10} + (\sigma_{11} + \sigma_{21})(\dot{y} - \dot{y}_{A1}) c_{10} & (\operatorname{sgn}(\Delta v_1) > 0) \\ -\sigma_{01}(x_0 - x_{A10}) s_{10} - (\sigma_{11} - \sigma_{21})(\dot{x} - \dot{x}_{A1}) s_{10} + \sigma_{01}(y_0 - y_{A10}) c_{10} + (\sigma_{11} - \sigma_{21})(\dot{y} - \dot{y}_{A1}) c_{10} & (\operatorname{sgn}(\Delta v_1) < 0) \\ 0 & (\operatorname{sgn}(\Delta v_1) = 0), \end{cases}$$

$$b = \begin{cases} \sigma_{02}(x_0 - x_{A20}) s_{20} + (\sigma_{12} + \sigma_{22})(\dot{x} - \dot{x}_{A2}) s_{20} - \sigma_{02}(y_0 - y_{A20}) c_{20} - (\sigma_{12} + \sigma_{22})(\dot{y} - \dot{y}_{A2}) c_{20} & (\operatorname{sgn}(\Delta v_2) > 0) \\ \sigma_{02}(x_0 - x_{A20}) s_{20} + (\sigma_{12} - \sigma_{22})(\dot{x} - \dot{x}_{A2}) s_{20} - \sigma_{02}(y_0 - y_{A20}) c_{20} - (\sigma_{12} - \sigma_{22})(\dot{y} - \dot{y}_{A2}) c_{20} & (\operatorname{sgn}(\Delta v_2) < 0) \\ 0 & (\operatorname{sgn}(\Delta v_2) = 0), \end{cases} \tag{18}$$

$$\alpha = \begin{cases} \sigma_{11} + \sigma_{21} & (\operatorname{sgn}(\Delta v_1) > 0) \\ \sigma_{11} - \sigma_{21} & (\operatorname{sgn}(\Delta v_1) < 0) \\ 0 & (\operatorname{sgn}(\Delta v_1) = 0), \end{cases}$$

$$\beta = \begin{cases} \sigma_{12} + \sigma_{22} & (\operatorname{sgn}(\Delta v_2) > 0) \\ \sigma_{12} - \sigma_{22} & (\operatorname{sgn}(\Delta v_2) < 0) \\ 0 & (\operatorname{sgn}(\Delta v_2) = 0). \end{cases}$$

Substitute the above equations into (13); we can get approximate model as follows:

$$M(q_0)\Delta\ddot{q} + H_7\Delta\dot{q} + (H_4 - H_1 - H_2 - H_5 - H_6)\Delta q = H_3 \begin{bmatrix} \Delta x_{A1} \\ \Delta y_{A1} \\ \Delta x_{A2} \\ \Delta y_{A2} \end{bmatrix}, \tag{19}$$

where

$$H_1 = \begin{bmatrix} 0 & 0 & F_{N_1}c_{10} & -F_{N_2}c_{20} \\ 0 & 0 & F_{N_1}s_{10} & -F_{N_2}s_{20} \\ 0 & 0 & 0 & 0 \\ 0 & 0 & 0 & 0 \end{bmatrix},$$

$$H_2 = \begin{bmatrix} -k_1s_{10}^2 - k_2s_{20}^2 & k_1s_{10}c_{10} + k_2s_{20}c_{20} & -k_1(x_0 - x_{A10})s_{10}c_{10} - k_1(y_0 - y_{A10})s_{10}^2 & k_2(x_{A20} - x_0)s_{20}c_{20} + k_2(y_{A20} - y_0)s_{20}^2 \\ k_1s_{10}c_{10} + k_2s_{20}c_{20} & -k_1c_{10}^2 - k_2c_{20}^2 & k_1(x_0 - x_{A10})c_{10}^2 + k_1(y_0 - y_{A10})s_{10}c_{10} & -k_2(x_{A20} - x_0)c_{20}^2 - k_2(y_{A20} - y_0)s_{20}c_{20} \\ k_1l_1s_{10} + k_1\delta_1c_{10} & -k_1l_1c_{10} + k_1\delta_1s_{10} & \mathfrak{A} & 0 \\ k_2l_2s_{20} - k_2\delta_2c_{20} & -k_2l_2c_{20} - k_2\delta_2s_{20} & 0 & \mathfrak{B} \end{bmatrix},$$

$$H_3 = \begin{bmatrix} k_1s_{10}^2 & -k_1s_{10}c_{10} & k_2s_{20}^2 & -k_2s_{20}c_{20} \\ -k_1s_{10}c_{10} & k_1c_{10}^2 & -k_2s_{20}c_{20} & k_2c_{20}^2 \\ -k_1l_1s_{10} - k_1\delta_1c_{10} & k_1l_1c_{10} - k_1\delta_1s_{10} & 0 & 0 \\ 0 & 0 & -k_2l_2s_{20} + k_2\delta_2c_{20} & k_2l_2c_{20} + k_2\delta_2s_{20} \end{bmatrix},$$

$$H_4 = \begin{bmatrix} 0 & 0 & 0 & 0 \\ 0 & 0 & 0 & 0 \\ 0 & 0 & -m_1gL_1s_{10} & 0 \\ 0 & 0 & 0 & -m_2gL_2s_{20} \end{bmatrix}, \tag{20}$$

$$H_5 = \begin{bmatrix} 0 & 0 & -F_{F_1}s_{10} & -F_{F_2}s_{20} \\ 0 & 0 & -F_{F_1}c_{10} & F_{F_2}c_{20} \\ 0 & 0 & 0 & 0 \\ 0 & 0 & 0 & 0 \end{bmatrix},$$

$$H_6 = \begin{bmatrix} -\sigma_{01}c_{10}^2 - \sigma_{02}c_{20}^2 & -\sigma_{01}s_{10}c_{10} - \sigma_{02}s_{20}c_{20} & -ac_{1_0} & bc_{20} \\ -\sigma_{01}s_{10}c_{10} - \sigma_{02}s_{20}c_{20} & -\sigma_{01}s_{10}^2 - \sigma_{02}s_{20}^2 & -as_{10} & bs_{20} \\ 0 & 0 & 0 & 0 \\ 0 & 0 & 0 & 0 \end{bmatrix},$$

$$H_7 = \begin{bmatrix} -\alpha c_{10}^2 - \beta c_{20}^2 & -\alpha s_{10}c_{10} - \beta s_{20}c_{20} & 0 & 0 \\ -\alpha s_{10}c_{10} - \beta s_{20}c_{20} & -\alpha s_{10}^2 - \beta s_{20}^2 & 0 & 0 \\ 0 & 0 & 0 & 0 \\ 0 & 0 & 0 & 0 \end{bmatrix},$$

where $\mathfrak{A}$ denotes $k_1l_1(x_0 - x_{A10})c_{10} + k_1l_1(y_0 - y_{A10})s_{10} - k_1\delta_1(x_0 - x_{A10})s_{10} + k_1\delta_1(y_0 - y_{A10})c_{10}$ and $\mathfrak{B}$ denotes $-k_2l_2(x_{A20} - x_0)c_{20} - k_2l_2(y_{A20} - y_0)s_{20} - k_2\delta_2(x_{A20} - x_0)s_{20} + k_2\delta_2(y_{A20} - y_0)c_{20}$.

We set $F_{F_i} = 0$ at equilibrium point, so H_5 is $0_{4\times4}$ and (19) can be represented as the following state equation:

$$\begin{aligned} \dot{\mathbf{x}} &= A\mathbf{x} + B\mathbf{u}, \\ \mathbf{y} - \mathbf{r} &= C\mathbf{x}, \end{aligned} \tag{21}$$

where

$$\mathbf{x} = (\Delta q \quad \Delta\dot{q})^T,$$

$$\mathbf{u} = (\Delta X_{A1} \quad \Delta Y_{A1} \quad \Delta X_{A2} \quad \Delta Y_{A2})^T,$$

$$A = \begin{bmatrix} 0_{4\times4} & I_{4\times4} \\ M^{-1}(q_0)(H_1 + H_2 + H_6 - H_4) & M^{-1}(q_0)H_7 \end{bmatrix},$$

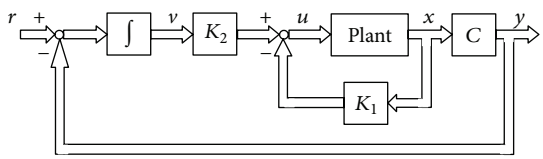

Figure 5: Block diagram of control system.

$$B = \begin{bmatrix} 0_{4\times4} \\ M^{-1}(q_0) H_3 \end{bmatrix},$$
$$C = \begin{bmatrix} I_{4\times4} & 0_{4\times4} \end{bmatrix}. \tag{22}$$

In order to guarantee the stability and tracking performance of the above plant, the control system is designed as shown in Figure 5. The above plant in (21) will be expanded to the following state equation:

$$\dot{\mathbf{x}}_\mathbf{e} = A_e \mathbf{x}_\mathbf{e} + B_e \mathbf{v}$$
$$\mathbf{y} - \mathbf{r} = \begin{bmatrix} C & 0_{4\times4} \end{bmatrix} \mathbf{x}_\mathbf{e}, \tag{23}$$

where

$$\mathbf{x}_\mathbf{e} = \begin{bmatrix} \mathbf{x} \\ \mathbf{u} \end{bmatrix}$$
$$A_e = \begin{bmatrix} A & B \\ 0_{4\times8} & 0_{4\times4} \end{bmatrix} \tag{24}$$
$$B_e = \begin{bmatrix} 0_{8\times4} \\ I_{4\times4} \end{bmatrix}.$$

Since $\operatorname{rank}([B_e \;\; A_e B_e]) = 12$, we know that plant (23) is controllable, and an optimal regulator can be designed for it. The cost function J is employed as

$$J = \int_0^\infty \left(\mathbf{x}_\mathbf{e}^T Q \mathbf{x}_\mathbf{e} + \mathbf{v}^T R \mathbf{v} \right) \mathrm{d}t, \tag{25}$$

where $Q > 0$ and $R > 0$. Then, optimal regulator which minimizes the cost function J is given as

$$\mathbf{v} = -K\mathbf{x}_\mathbf{e} = -R^{-1} B_e^T P \mathbf{x}_\mathbf{e}, \tag{26}$$

where P is the solution of the following Riccati equation:

$$PA_e + A_e^T P - PB_e R^{-1} B_e^T P + Q = 0. \tag{27}$$

So, K_1 and K_2 can be derived as

$$\begin{bmatrix} K_1 & K_2 \end{bmatrix} = K \begin{bmatrix} A & B \\ C & 0_{4\times4} \end{bmatrix}^{-1}. \tag{28}$$

According to (18), we can see that A will vary along with the variations of H_6 and H_7. That means parameters K_1 and K_2 of the designed optimal regulator will also vary simultaneously.

Table 1: Parameters of the system.

	$i = 1$	$i = 2$
m_i [Kg]	2.71	2.5
L_i [m]	0.367	0.399
I_i [Kg·m^2]	0.17	0.136
r_i [m]	0.051	0.051
k_i [N/m]	10^5	10^5
d_i [N·s/m]	10^3	10^3
σ_{0i} [N/m]	10	10
σ_{1i} [N·s/m]	0.1	0.1
σ_{2i} [N·s/m]	0.001	0.001
μ_{Ci}	0.08	0.08
μ_{Si}	0.161	0.161
$v_{\mathrm{st}i}$ [m/s]	0.01	0.01

5. Simulation Results

In this section, by using the above proposed optimal regulator, simulation for holding two-rigid-link object at the same place was done. The initial state of the object is $q_0 = \left(-0.029\,[\mathrm{m}] \;\; -0.234\,[\mathrm{m}] \;\; 150.4^\circ \;\; 29.8^\circ\right)^T$ and the desired state is $q_r = \left(-0.03\,[\mathrm{m}] \;\; -0.235\,[\mathrm{m}] \;\; 150^\circ \;\; 30^\circ\right)^T$. In this simulation, q_r is regarded as equilibrium point and initial positions of two arms are obtained as $u_0 = \left(-0.3033\,[\mathrm{m}] \;\; -0.1357\,[\mathrm{m}] \;\; 0.2441\,[\mathrm{m}] \;\; -0.1353\,[\mathrm{m}]\right)^T$. The parameters of the system are shown in Table 1. The total time of simulation is $T = 7\,[\mathrm{s}]$, and $F_d = \left(0\,[\mathrm{Kgf}] \;\; -0.1\,[\mathrm{Kgf}]\right)^T$ is added as disturbance to the joint of the two-rigid-link object during $t = 2 \sim 2.1\,[\mathrm{s}]$. For optimal regulator, we chose $Q_1 = \mathrm{diag}\{40, 20, 2, 4, 0.4, 0.2, 0.02, 0.04, 2, 2, 2, 2\}$, $R_1 = \mathrm{diag}\{7.5, 7.5, 7.5, 7.5\}$ and $Q_2 = \mathrm{diag}\{200, 100, 10, 20, 2, 1, 0.1, 0.2, 10, 10, 10, 10\}$, $R_2 = \mathrm{diag}\{5, 5, 5, 5\}$ for comparison. The simulation results are shown as in Table 1.

In Figure 6, dashed lines show the position (x, y) of the object's joint and orientation angles (θ_1, θ_2) of the object with Q_1 and R_1, solid lines show the ones with Q_2 and R_2, and dotted lines show the desired position $(x_{\mathrm{ref}}, y_{\mathrm{ref}})$ and orientation angles $(\theta_{1\mathrm{ref}}, \theta_{2\mathrm{ref}})$. From Figure 6, we can see the position of the object's joint and the orientation angles of the object are controlled to be stable on the desired state; even a disturbance F_d was added during $t = 2 \sim 2.1\,[\mathrm{s}]$. Figure 7 shows the positions of two arms with different Q and R during stabilizing the object. Since we set the initial positions of two arms as the ones which can make the system be equilibrium on the desired state, we can see two arms were moved to try to keep the object at the beginning. After being disturbed by F_d, two arms began to move again to stabilize the object. Finally the object was stabilized and kept on the desired state. In Figures 8 and 9, the variations of parameters K_1^T and K_2^T during $t = 1{\sim}4\,[\mathrm{s}]$ by using Q_2 and R_2 are shown. We can see that the parameters of the designed optimal regulator varied during holding motion of two cooperative arms for guaranteeing the stability of the whole system.

From the above simulation results, the effectiveness of the proposed method is verified. Also, we know that making Q

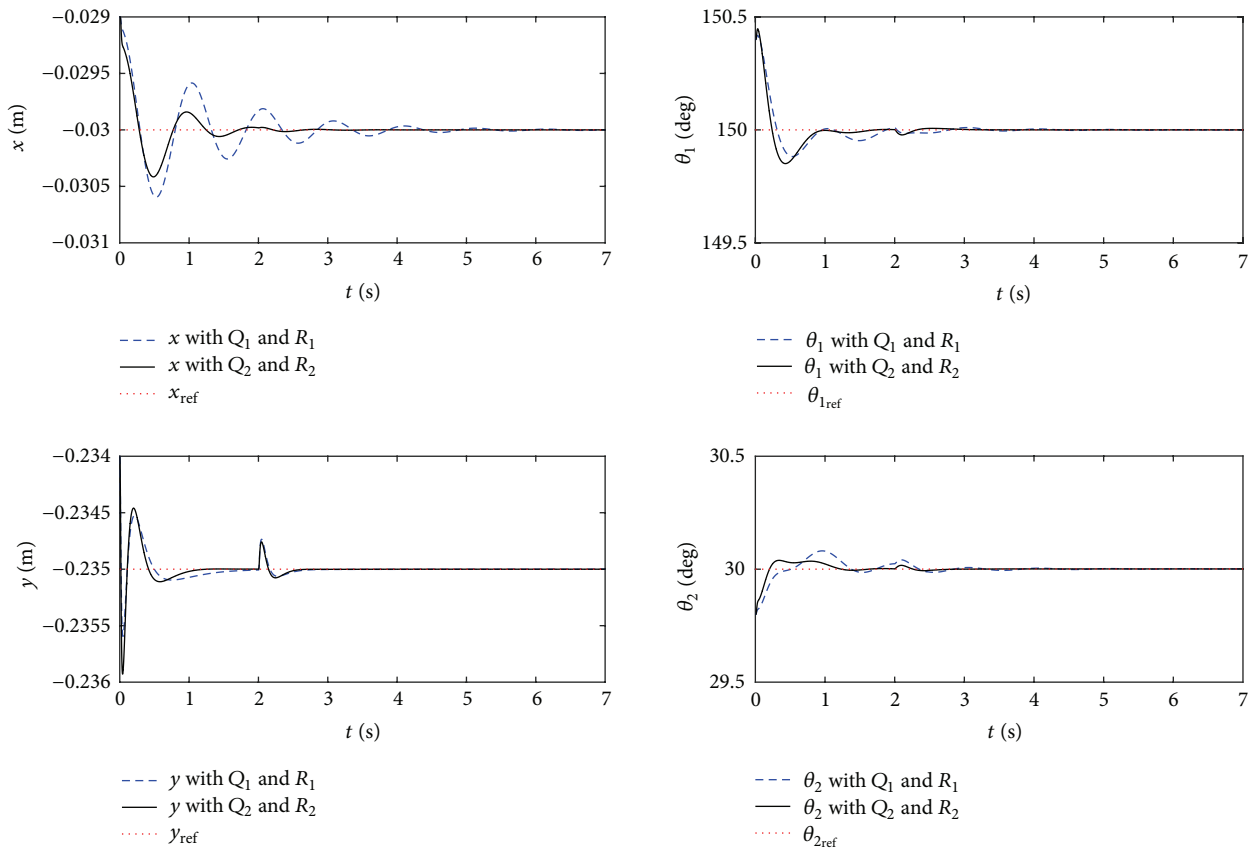

FIGURE 6: State of the two-rigid-link object.

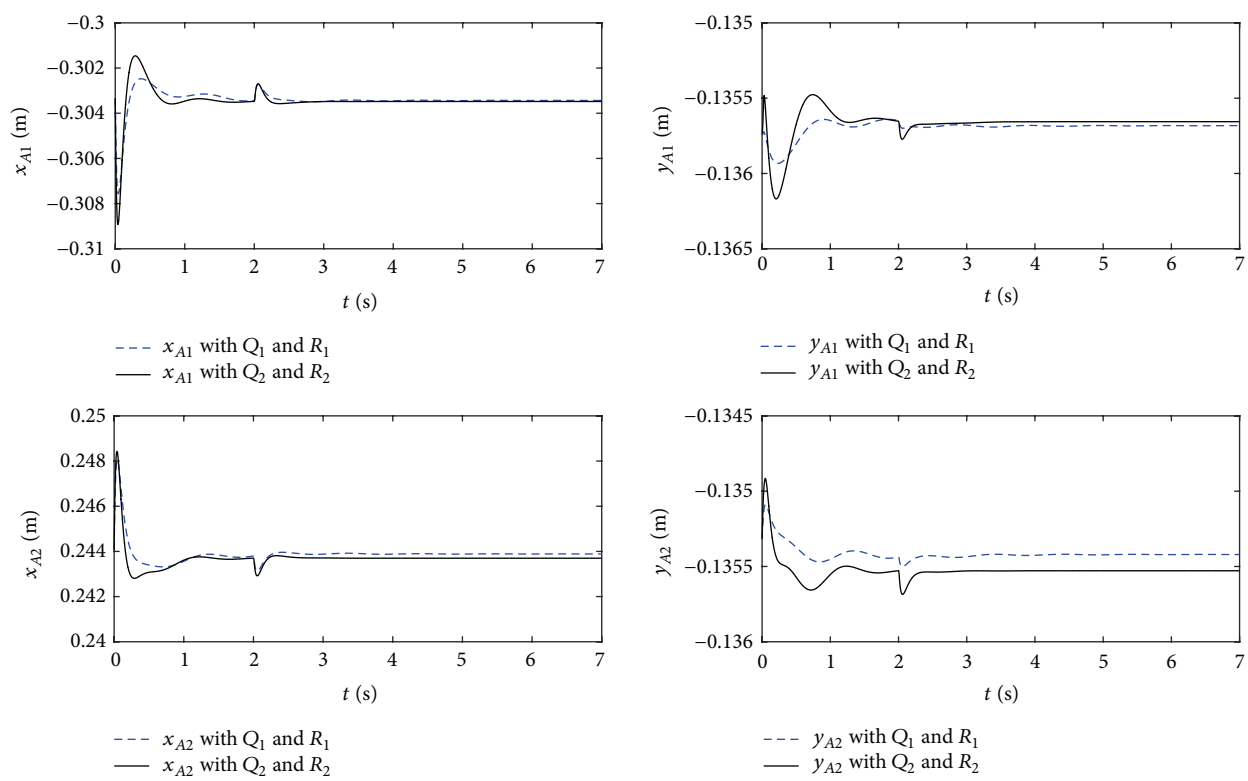

FIGURE 7: Positions of two arms.

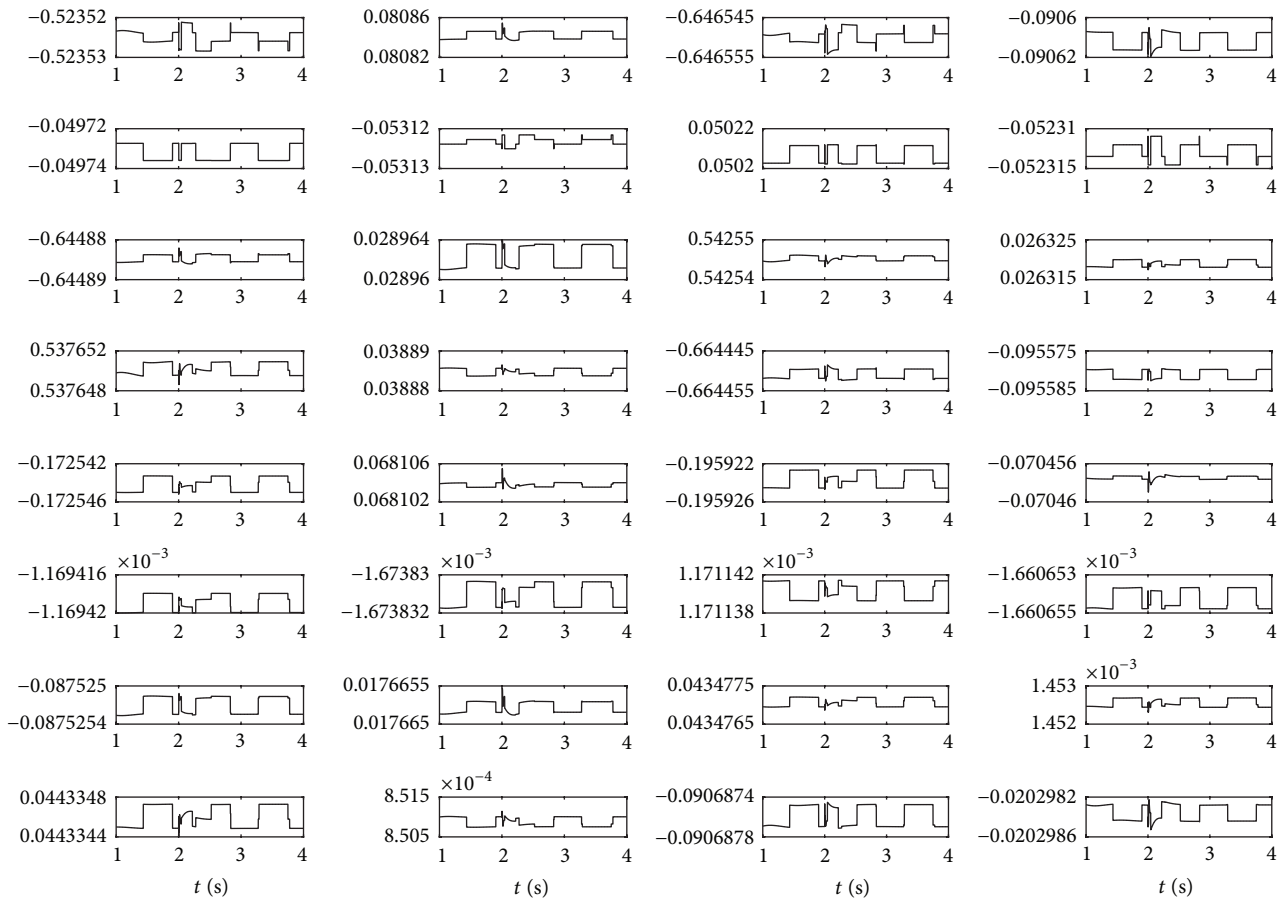

Figure 8: Parameter K_1^T.

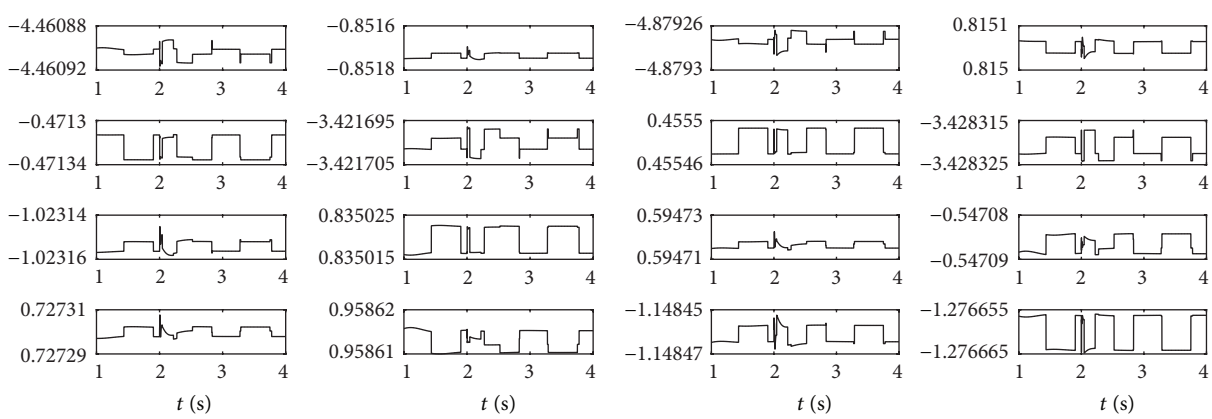

Figure 9: Parameter K_2^T.

bigger and R smaller can improve response of this system. That means in the future work, for avoiding leading care-receiver to feel afraid, uncomfortable, and even pained, it is feasible to modify the movement of two-cooperative-arm robot according to the feeling of the care-receiver by changing Q and R.

Further, by using the same parameters as above, we compared the simulation results between our proposed method and the one of [18] which did not consider friction in dynamic model of the system. In Figure 10, the states of the two-rigid-link object with and without considering friction are shown. Since the friction is small, two results are nearly the same. Then, we changed the parameters of friction to $\sigma_{0i} = 101$, $\sigma_{1i} = 1$, and $\sigma_{2i} = 0.01$ to make the friction bigger and obtained Figure 11. From Figure 11, we can see that the tracking performance of the position (solid lines) of the object with our proposed method is better than the one (dashed lines) with the method of [18], and the speeds

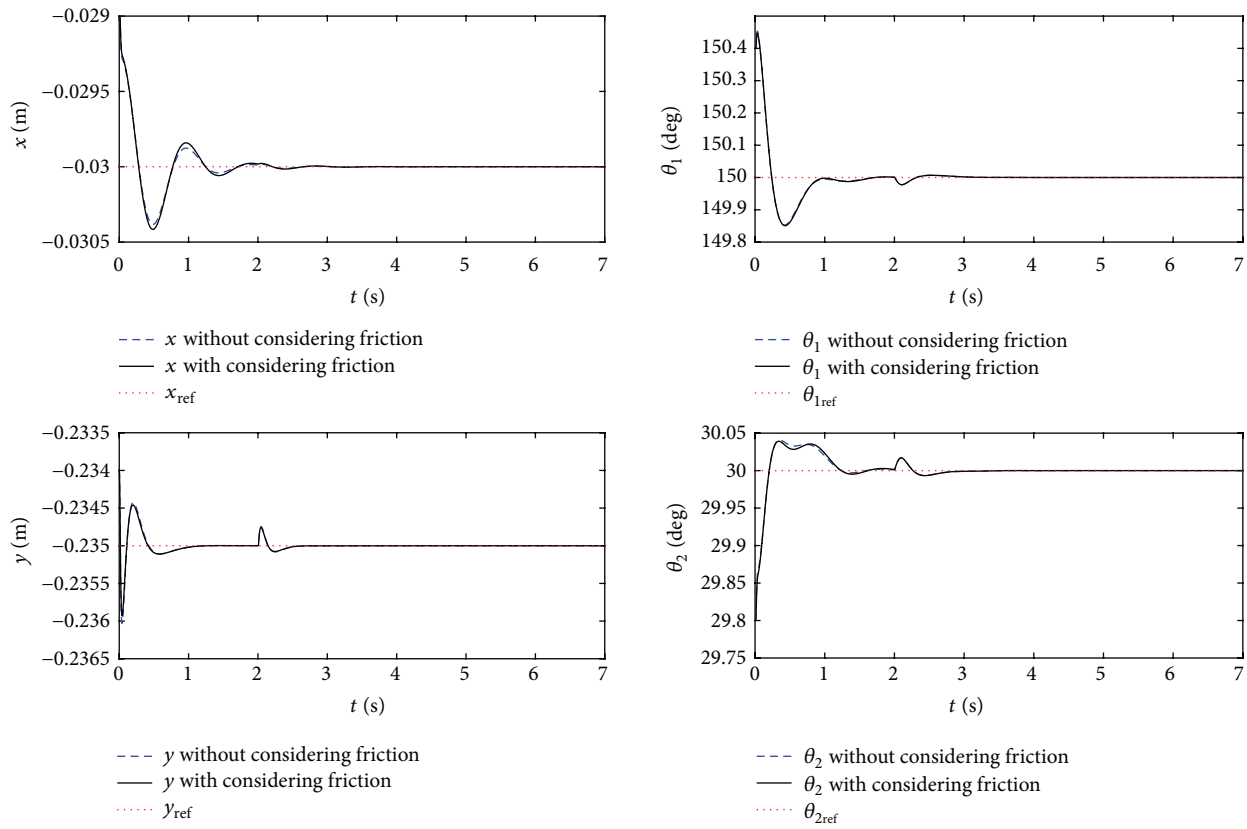

Figure 10: State of the two-rigid-link object.

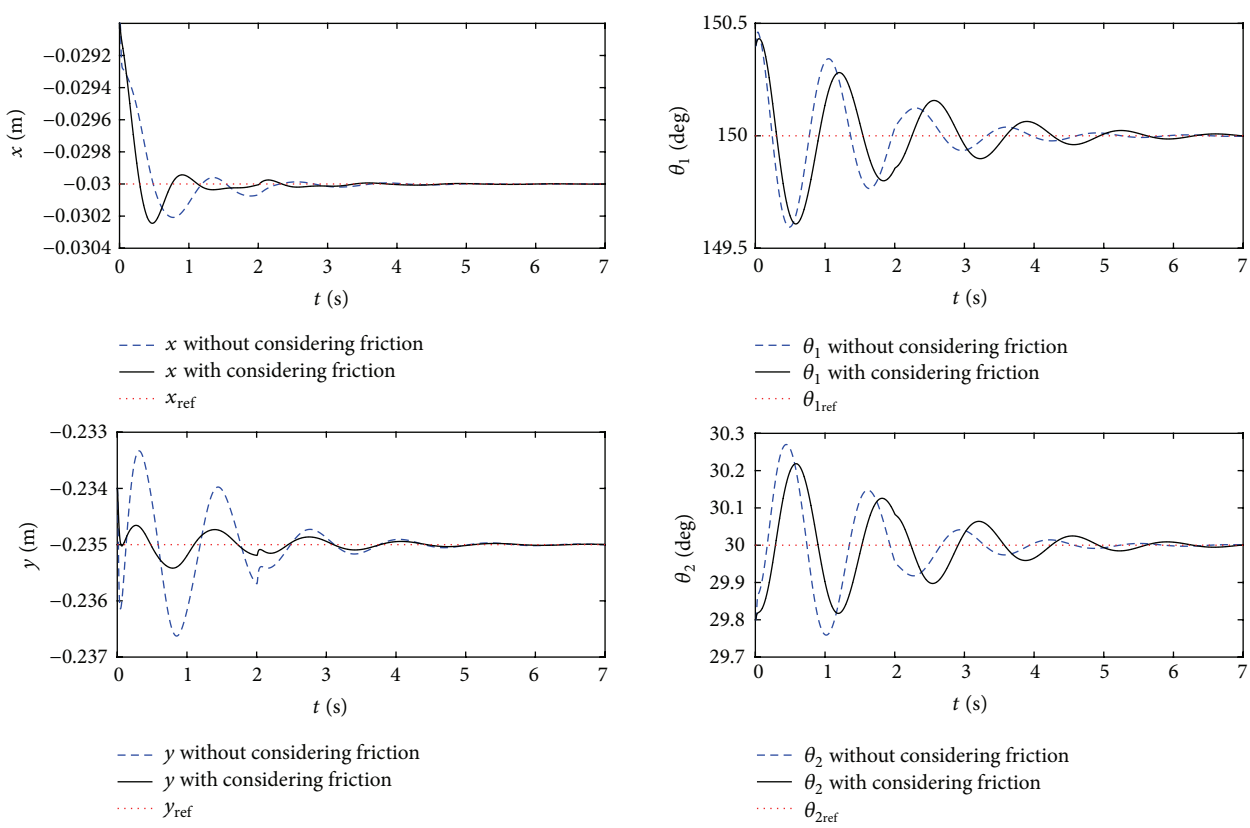

Figure 11: State of the two-rigid-link object with different friction.

of convergence of the orientation angles (solid lines) of the object with our proposed method are a little later than the one (dashed lines) with the method of [18]. In practice, since the effect of the friction could not be small enough to be ignored, the friction should be considered in the dynamic model of the system. The effectiveness of our proposed method to control the holding motion of two-cooperative-arm robot with considering friction is verified by the above simulation results.

6. Conclusion

In this paper, an approximate model of a two-rigid-link object which is regarded as a care-receiver was obtained based on its dynamic model including viscoelastic model and LuGre model for interaction behavior between object and robot arms. For guaranteeing the stability and tracking performance of the considered system, an optimal regulator was designed to realize the holding motion of two cooperative arms. In order to show the effectiveness of the designed optimal regulator, simulation results were given. The feasibility of modifying the movement of two-cooperative-arm robot by changing Q and R of the designed optimal regulator was also shown.

Competing Interests

The authors declare that they have no competing interests.

Acknowledgments

The first author would like to thank RIKEN of Japan for giving him the chance to carry out one part of this research work during his term as a Researcher at RIKEN-SRK Collaboration Center for Human-Interactive Robot Research and thank Professor Y. Hayakawa at Nagoya University for his suggestions and comments.

References

[1] W. Mori, J. Ueda, and T. Ogasawara, "1-DOF dynamic pitching robot that independently controls velocity, angular velocity, and direction of a ball: contact models and motion planning," in *Proceedings of the IEEE International Conference on Robotics and Automation (ICRA '09)*, pp. 1655–1661, Kobe, Japan, May 2009.

[2] M. Higashimori, K. Utsumi, Y. Omoto, and M. Kaneko, "Dynamic manipulation inspired by the handling of a pizza peel," *IEEE Transactions on Robotics*, vol. 25, no. 4, pp. 829–838, 2009.

[3] B. Beigzadeh, M. N. Ahmadabadi, and A. Meghdari, "Two dimensional dynamic manipulation of a disc using two manipulators," in *Proceedings of the IEEE International Conference on Mechatronics and Automation (ICMA '06)*, pp. 1191–1196, Luoyang, China, June 2006.

[4] A. Gupta and W. H. Huang, "A carrying task for nonprehensile mobile manipulators," in *Proceedings of the IEEE/RSJ International Conference on Intelligent Robots and Systems*, pp. 2896–2901, IEEE, Las Vegas, Nev, USA, October 2003.

[5] M. Onishi, T. Odashima, and Z. Luo, "Emergent cooperative manipulation of a multi-linked object," in *Proceedings of the SICE 2003 Annual Conference*, vol. 3, pp. 3049–3052, IEEE, Fukui, Japan, 2003.

[6] Z. Zyada, Y. Hayakawa, and S. Hosoe, "Model-based control for nonprehensile manipulation of a two-rigid-link object by two cooperative arms," in *Proceedings of the IEEE International Conference on Robotics and Biomimetics (ROBIO '10)*, pp. 472–477, Tianjin, China, December 2010.

[7] Z. Zyada, Y. Hayakawa, and S. Hosoe, "Fuzzy nonprehensile manipulation control of a two-rigid-link object by two cooperative arms," in *Proceedings of the 18th IFAC World Congress*, vol. 44, pp. 14614–14621, Milano, Italy, 2011.

[8] C. Jiang, S. Hirano, Y. Hayakawa, T. Suzuki, and S. Hosoe, "Non-prehensile manipulation control by two cooperative arms without compensating friction," in *Proceedings of the 20th International Conference on Electrical Engineering*, pp. 1950–1954, 2014.

[9] F. L. Lewis, D. M. Dawson, and C. T. Abdallah, *Robot Manipulator Control: Theory and Practice*, Marcel Dekker, New York, NY, USA, 2004.

[10] C.-S. Kim, E.-J. Mo, S.-M. Han, M.-S. Jie, and K.-W. Lee, "Robust visual servo control of robot manipulators with uncertain dynamics and camera parameters," *International Journal of Control, Automation and Systems*, vol. 8, no. 2, pp. 308–313, 2010.

[11] M. Deng, N. Bu, and A. Inoue, "Output tracking of nonlinear feedback systems with perturbation based on robust right coprime factorization," *International Journal of Innovative Computing, Information and Control*, vol. 5, no. 10, pp. 3359–3366, 2009.

[12] A. Wang and M. Deng, "Operator-based robust nonlinear tracking control for a human multi-joint arm-like manipulator with unknown time-varying delays," *Applied Mathematics and Information Sciences*, vol. 6, no. 3, pp. 459–468, 2012.

[13] M. Deng and N. Bu, "Robust control for nonlinear systems using passivity-based robust right coprime factorization," *IEEE Transactions on Automatic Control*, vol. 57, no. 10, pp. 2599–2604, 2012.

[14] A. Wang and M. Deng, "Robust nonlinear control design to a manipulator based on operator based approach," *ICIC Express Letters*, vol. 6, no. 3, pp. 617–623, 2012.

[15] P. Tomei, "Adaptive PD controller for robot manipulators," *IEEE Transactions on Robotics and Automation*, vol. 7, no. 4, pp. 565–570, 1991.

[16] C.-J. Chien and A. Tayebi, "Further results on adaptive iterative learning control of robot manipulators," *Automatica*, vol. 44, no. 3, pp. 830–837, 2008.

[17] S. Islam and X. P. Liu, "Robust sliding mode control for robot manipulators," *IEEE Transactions on Industrial Electronics*, vol. 58, no. 6, pp. 2444–2453, 2011.

[18] C. Jiang, S. Ueno, and Y. Hayakawa, "Optimal control of nonprehensile manipulation control by two cooperative arms," in *Proceedings of the International Conference on Advanced Mechatronic Systems (ICAMechS '15)*, pp. 533–537, Beijing, China, August 2015.

[19] C. Canudas de Wit, H. Olsson, K. J. Åström, and P. Lischinsky, "A new model for control of systems with friction," *IEEE Transactions on Automatic Control*, vol. 40, no. 3, pp. 419–425, 1995.

[20] M. Sasaki and M. Okugawa, "Motion control of a piezopolymer bimorph flexible microactuator," *Journal of Robotics and Mechatronics*, vol. 7, no. 6, pp. 467–473, 1995.

[21] RIKEN, "Introduction of ROBEAR," http://rtc.nagoya.riken.jp/ROBEAR/.